Magnetoswitching of current oscillations in dilute magnetic semiconductor nanostructures

R. Escobedo,[1] M. Carretero,[2,3] L. L. Bonilla,[2,3] and G. Platero[4]
[1]*Departamento de Matemática Aplicada y Ciencias de la Computación, Universidad de Cantabria, 39005 Santander, Spain*
[2]*G. Millán Institute, Fluid Dynamics, Nanoscience and Industrial Mathematics, Universidad Carlos III de Madrid, 28911 Leganés, Spain*
[3]*Unidad Asociada al Instituto de Ciencia de Materiales de Madrid, CSIC, 28049 Cantoblanco, Madrid, Spain*
[4]*Instituto de Ciencia de Materiales de Madrid, CSIC, 28049 Cantoblanco, Madrid, Spain*
(Received 15 July 2009; revised manuscript received 10 September 2009; published 13 October 2009)

Strongly nonlinear transport through dilute magnetic semiconductor multiquantum wells occurs due to the interplay between confinement, Coulomb, and exchange interaction. Nonlinear effects include the appearance of spin-polarized stationary states and self-sustained current oscillations as possible stable states of the nanostructure, depending on its configuration and control parameters such as voltage bias and level splitting due to an external magnetic field. Oscillatory regions grow in size with well number and level splitting. A systematic analysis of the charge and spin response to voltage and magnetic field switching of II-VI dilute magnetic semiconductor multiquantum wells is carried out. The description of stationary and time-periodic spin-polarized states, the transitions between them and the responses to voltage or magnetic field switching have great importance due to the potential implementation of spintronic devices based on these nanostructures.

DOI: 10.1103/PhysRevB.80.155202 PACS number(s): 75.50.Pp, 85.75.−d, 72.25.Dc, 73.63.Hs

I. INTRODUCTION

Spin injection is one of the aims of spintronics[1] thanks to the potential applications of injectors as spin light-emitting diode devices, etc. Also quantum state transfer from spin electrons to photons by interband transitions is actively investigated.[2–4] One of the most efficient ways of spin injection to date[5,6] is the use of II-VI dilute magnetic semiconductors (DMSs) that exhibit the giant Zeeman effect:[7] they have a conductivity comparable to that of nonmagnetic semiconductors and can boast spin polarizations close to 100% at a small applied magnetic field. However, spin-injection experiments in semiconductors enter easily the regime of nonlinear response.[8] Different effects could contribute to nonlinear transport and therefore to nonlinear spin injection. For example, band bending effects[9] in nanostructures give rise to a nonlinear current due to the interplay between Coulomb interaction and electron tunnel in these confined systems, which have quasidiscrete states.

Other physical mechanisms inherent to these systems explain their current-voltage characteristics: for instance, a large Zeeman level splitting Δ in an applied magnetic field B. Recently, spin transport through DMS diodes[10] and multiquantum well structures (MQWSs) has been analyzed.[11–14] These works study nonlinear features of the current (hysteresis and multistability) as a function of the external voltage. Under strong dc voltage bias V, electric field domains are formed in MQWS due to the interplay between electron-electron interaction and resonant tunneling.[11] In other sample configurations or, for different doping density, there are spin-polarized self-sustained current oscillations (SSCOs) and the system could behave as a spin oscillator.[12,13] To tailor the properties of these spin oscillators or injectors, it is important to perform a systematic analysis of the transition from stationary to time dependent current, in terms of sample configuration, external magnetic field, doping density, etc.

In this paper we analyze the response to voltage (V) or magnetic (B) switching in a n-doped dc voltage biased semiconductor MQWS having its first quantum well (QW) doped with Mn. Both spin-polarized stationary states (SSs) and SSCOs are possible stable states of the MQWS for different values of the parameters. Stationary states field profiles consist of two electric field domains separated by a domain wall which is a charge monopole.[14] Magnetic field switching requires knowing phase diagrams of the current density J and the applied voltage V versus the level splitting Δ (due to the magnetic field B), and these diagrams are among the results of this paper. The phase diagram of V versus Δ shows regions of stable SSCOs embedded in others of stable SSs. The extension of the SSCO regions increases with the number of QWs in the structure. Sudden changes in V or B may switch or disconnect SSCOs from an initial stable SS or force the domain wall to change its location. The SSCOs are due to periodic triggering of charge dipoles at the Mn-doped well and their motion toward the collector.[13] Large level splitting induced by B due to the exchange interaction provides DMS MQWSs with a new degree of freedom which is absent in conventional III-V weakly coupled n-doped semiconductor MQWSs.[15] Another important difference is that, in the latter, both charge dipoles and monopoles may be triggered at the injector (depending on its current-field characteristics: its conductivity if the relation between current and field is linear) and both may cause SSCOs.[15,16] In these materials and for moderate conductivity of the injecting contact, switching the voltage V between different SSs involves either upward monopole motion or a dipole-tripole mechanism.[15,17,18] For sufficiently large conductivity of the injector, the dipole-tripole mechanism ceases to exist and voltage switching involves injection of a charge monopole that moves toward the collector until it reaches the QW corresponding to the final stable SS.[19] Voltage or magnetic switching in II-VI MQWSs always involves dipole nucleation at the Mn-doped QW.

II. MODEL

Our sample configuration consists of an n-doped ZnSe/(Zn,Cd,Mn)Se weakly coupled MQWS. The spin for the

magnetic ion Mn^{++} is $S=5/2$ and the exchange interaction between the Mn local moments and the conduction-band electrons is ferromagnetic in II-VI QWs. The energy spectrum corresponding to N isolated QWs comprising our weakly coupled MQWS has the form $E_j+\hbar^2k_\perp/(2m^*)$, where m^* is the effective mass, $k_\perp$ is the in-plane wave vector orthogonal to the growth direction and $j=1,\ldots,N$ is the QW subband index. In the weak magnetic fields considered here, we disregard Landau-level formation and $k_\perp$ is a continuous variable.[11] Using the virtual-crystal and mean-field approximations, the exchange interaction causes the subband energies to depend on spin in those QWs containing Mn ions,

$$E_j^{\pm} = E_j \mp \Delta/2, \tag{1}$$

where

$$\Delta(B) = 2J_{sd}N_{Mn}SB_S\left(\frac{g\mu_B S}{k_B T_{eff}}B\right) \tag{2}$$

for spin $s=\pm 1/2$, and B_S, J_{sd}, N_{Mn}, and T_{eff} are the Brillouin function, the exchange integral, the density of magnetic impurities, and an effective temperature which accounts for Mn interactions, respectively.[11,20]

We model spin-flip scattering coming from spin-orbit or hyperfine interaction by a phenomenological scattering time τ_{sf}, which is larger than impurity and phonon-scattering times: $\tau_{scat}<\tau_{sf}$. Vertical transport in the weakly coupled MQWS is spin-independent sequential tunneling between adjacent QWs so that when electrons tunnel to an excited state they instantaneously relax by phonon scattering to the ground state, with the same spin polarization.[11] Lastly, electron-electron interaction is considered within the Hartree mean-field approximation.

The equations governing the model are[13,14] the discrete Poisson equation relating the two-dimensional (2D) spin-up and spin-down electron densities, n_i^+ and n_i^-, respectively, to the average electric field $-F_i$ at the ith MQWS period (of length l),

$$\varepsilon(F_i - F_{i-1}) = e(n_i^+ + n_i^- - N_D) \tag{3}$$

and the rate equations for $n_i^{\pm}$,

$$e\frac{dn_i^{\pm}}{dt} = J_{i-1\to i}^{\pm} - J_{i\to i+1}^{\pm} \pm \frac{A(n_i^+,n_i^-,\mu_i^+)}{\tau_{sf,i}}, \tag{4}$$

for $i=1,\ldots,N$. For numerical convenience, we have introduced here a smoothed form $A(n_i^+,n_i^-,\mu_i^+)$ of the scattering term used in Ref. 11 given by

$$A(n_i^+,n_i^-,\mu_i^+) = n_i^- - \frac{n_i^+}{1+\exp\left(\frac{E_{1,i}^- - \mu_i^+}{\gamma_\mu}\right)}, \tag{5}$$

where γ_μ is a small smoothing parameter (smaller than $\gamma=\hbar/\tau_{scatt}$ or than the thermal energy) such that, as $\gamma_\mu\to 0$,

$$\pm A(n_i^+,n_i^-,\mu_i^+) \to \pm n_i^- + \begin{cases} \mp n_i^+ & \text{for } \mu_i^+ > E_{1,i}^- \\ 0 & \text{otherwise} \end{cases},$$

which was used by Sánchez *et al.*[11] (note that $\mu_i^+ > E_{1,i}^-$ is equivalent to $\mu_i^+ - E_{1,i}^+ > \Delta$).

In these expressions, $\mu_i^{\pm}$ is the chemical potential at the ith MQWS period and $E_{j,i}^{\pm}$ are the spin-dependent subband energies (measured from the bottom of the ith well): $E_{j,1}^{\pm} = E_j \mp \Delta/2$ and $E_{j,i}^{\pm} = E_j$ for $i\neq 1$. Also, N_D and ε are the 2D doping density at the QWs and the average permittivity.

In weakly coupled MQWS, tunneling between adjacent QWs can be treated in leading-order perturbation theory. Since elastic and inelastic-scattering times in the QWs are shorter than any other time scale of the problem, we can assume that the electrons in each well are in quasi-equilibrium between successive tunneling events and that their temperature is that of the lattice. We ignore interwell spin-flip processes so that currents are carried between wells by the two spin subsystems in parallel. Then, as in the case of nonmagnetic MQWSs, the tunneling current densities across the ith barrier $J_{i\to i+1}^{\pm}$ can be calculated by the Bardeen transfer Hamiltonian method.[21–24] See the detailed derivation for nonmagnetic MQWSs in Ref. 19. The well-known resulting expression[19,25] can be approximated by the formula[14]

$$J_{i\to i+1}^{\pm} = \frac{ev^{(f)\pm}(F_i)}{l}\left\{n_i^{\pm} - \frac{m^*k_BT}{2\pi\hbar^2}\ln\left\{1+e^{-eF_il/k_BT} \times \left[\exp\left(\frac{2\pi\hbar^2 n_{i+1}^{\pm}}{m^*k_BT}\right)-1\right]\right\}\right\}, \tag{6}$$

where $i=1,\ldots,N-1$, provided that scattering-induced broadening of energy levels is much smaller than subband energies and chemical potentials; see Appendix A of Ref. 25. The spin-dependent "forward tunneling velocity," $v^{(f)\pm}$, is a sum of Lorentzians of width 2γ, with $\gamma=\hbar/\tau_{scatt}$ (the same value for all subbands, for simplicity), centered at the resonant field values $F_{j,i}^{\pm}=(E_{j,i+1}^{\pm}-E_{1,i}^{\pm})/(el)$,

$$v^{(f)\pm}(F_i) = \frac{\hbar^3 l\gamma}{2\pi^2 m^{*2}}\sum_{j=1}^{2}\frac{\mathcal{T}_i(E_{1,i}^{\pm})}{(F_i - F_{j,i}^{\pm})^2(el)^2 + (2\gamma)^2}, \tag{7}$$

where $\mathcal{T}_i$ is proportional to the transmission coefficient of the ith barrier.[25] For electrons with spin $\pm 1/2$, the chemical potential $\mu_i^{\pm}$ and the electron densities $n_i^{\pm}$ are related by

$$n_i^{\pm} = \frac{m^*k_BT}{2\pi\hbar^2}\ln\left[1+\exp\left(\frac{\mu_i^{\pm}-E_{1,i}^{\pm}}{k_BT}\right)\right]. \tag{8}$$

The voltage bias condition can be written as

$$\sum_{i=0}^{N} F_i l = V. \tag{9}$$

Defining $J_{i\to i+1}=J_{i\to i+1}^+ + J_{i\to i+1}^-$, the total current density $J(t)$ can be calculated as

$$J(t) = \frac{1}{N+1}\sum_{i=0}^{N} J_{i\to i+1}. \tag{10}$$

Then, time differencing the Poisson equation, inserting the rate equations for $n_i^{\pm}$ in the result, and assuming a constant applied voltage ($dV/dt=0$), we obtain the following equation relating $F_i(t)$, $J_{i\to i+1}(t)$, and $J(t)$ for $i=0,\ldots,N$,

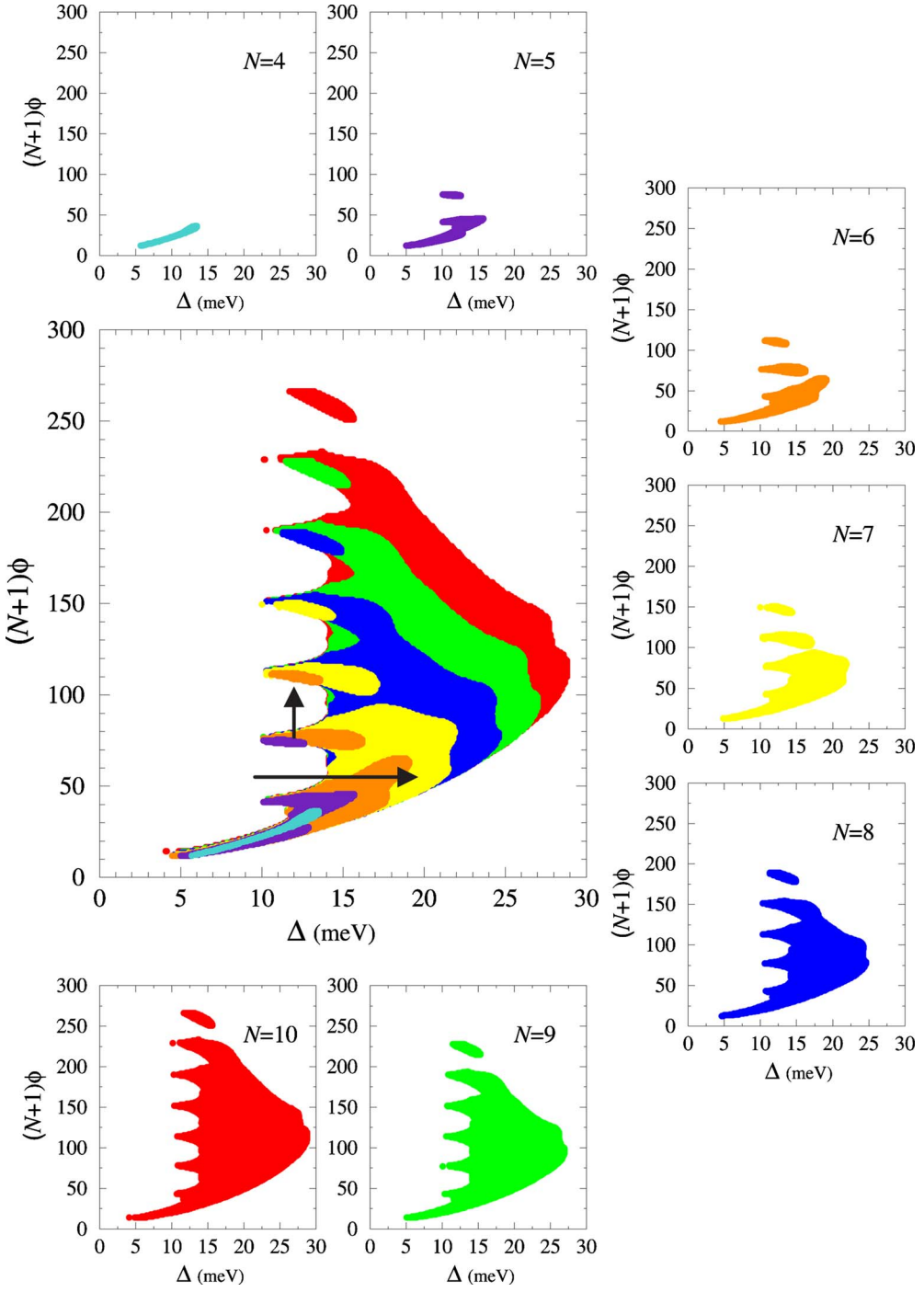

FIG. 1. (Color online) Central panel: phase diagram of dimensionless voltage $(N+1)\phi=V/V_0$ ($V_0=0.96$ mV) versus Δ for different N. Lateral panels: same phase diagram but for specific values of $N=4,5,6,7,8,9,10$. The SS is stable in the white region, whereas SSCOs are stable in the shaded (colored) regions. For a given value of N, the SSCO regions contain those for all smaller values of N.

$$\varepsilon\frac{dF_i}{dt}+J_{i\to i+1}=J(t). \tag{11}$$

Boundary tunneling currents for $i=0$ and $i=N$ are determined by using tunneling currents with $n_0^{\pm}=n_{N+1}^{\pm}=N_D/2$ (identical normal contacts).[11]

As initial conditions, we set $n_i^{\pm}=N_D/2$ (normal QWs) and $F_i=\phi F_M$, where F_M is a reference field corresponding to the first local maximum (F_M,J_M) of the tunneling current $J_{i\to i+1}(F,n_i^+,n_i^-,n_{i+1}^+,n_{i+1}^-)$ for $n_i^{\pm}=n_{i+1}^{\pm}=N_D/2$ in a nonmagnetic well,[14] and ϕ is a dimensionless average field defined by

$$\phi=\frac{V}{l(N+1)F_M}. \tag{12}$$

$(N+1)\phi$ is the dimensionless voltage across the MQWS.

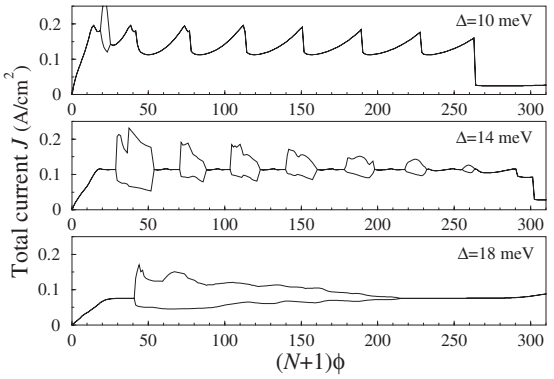

FIG. 2. *J-V* characteristic curves for a MQWS with $N=10$ and level splittings of $\Delta=10$, 14, and 18 meV.

III. RESULTS

We have considered barrier and QW widths of 10 and 5 nm, respectively, $\tau_{sf}=10^{-9}$ s (normal QW) and 10^{-11} s (magnetic QW), $m^*=0.16m_0$, $N_D=10^{10}$ cm^{-2}, $\varepsilon=7.1\varepsilon_0$, $T=5$ K, $E_1=15.76$ meV, $E_2=61.99$ meV, $\gamma=1$ meV, and $\gamma_\mu=0.1$ meV.[13]

To find the relation between Δ and B, we used the values $g=2$, $S=5/2$, and $T_{\text{eff}}=T+T_0$ with $T_0=2$ K. The prefactor in Eq. (2) can be estimated from Fig. 3 of Ref. 20 to be 23.26 meV. Then, for $T=5$ K, we find

$$\Delta(B) = 23.26B_{5/2}(B/2.084), \tag{13}$$

units of B and Δ are Tesla and meV, respectively.

Figure 1 depicts the phase diagram of voltage versus B-induced level splitting Δ. We observe that the extension of the parameter regions corresponding to SSCOs increases with N, the number of QWs in the structure, and that SSCO regions for a fixed N contain SSCO regions for structures with smaller N. To the left of the main oscillatory regions there are sometimes small oscillatory regions which appear as isolated dots in Fig. 1. Whether these dots are connected to the main oscillatory regions by extremely thin regions (narrower than the discretization error of the code) is something our numerical solution of the model has not been able to decide. Even though these connecting regions have not been found and therefore they are not shown in the figure, we cannot discard their existence. In fact the dots are absorbed by the larger oscillatory regions to their right as N increases.

Figure 2 shows the total current density $J(t)$ as a function of the applied dimensionless voltage ϕ for $N=10$. In agreement with Fig. 1, we observe that the width of SSCO regions increases with Δ. For intermediate values of Δ, the number of oscillatory regions first increases and then decreases again when the oscillatory regions merge for larger Δ.

The phase diagram shows similar features if we change Δ at fixed V: there is only one finite interval of SSCOs, (Δ_l,Δ_u), cf. Fig. 1. In terms of the magnetic field B, the situation is somewhat different. The level splitting Δ is given by a Brillouin function of B, so Δ can only take on values smaller than a saturating value, Δ_∞. If $\Delta_u<\Delta_\infty$, there may be SSCOs for a finite interval of B as shown in Fig. 3 or for an infinite interval if $\Delta_\infty<\Delta_u$ (inset of Fig. 3).

The MQWS response to a sudden switching of the voltage or the magnetic field can be inferred from Fig. 1. Let us increase ϕ at fixed Δ as indicated by the vertical arrow in Fig. 1 (from SSCOs to SSs). After a transient, the MQWS settles to the SS, as shown in Figs. 4(a) and 4(b). The periodic generation of a high-field domain at the magnetic QW $i=1$ and its motion toward the high-field region adjacent to the collector yield SSCOs (Panel b). The transient corresponds to the nucleation of a last and larger high-field domain at the first QW and its motion until its trailing domain wall reaches the location corresponding to the stable SS (cf. the similar dipole-tripole mechanism in Refs. 15, 17, and 18). Increasing abruptly ϕ between SSs in different regions of Fig. 1 always involves dipole emission at the magnetic QW, unlike the one-well upward domain-wall motion possible in conventional III-V MQWS.[17]

For fixed ϕ, a sudden increment of B from a stable SS region to a SSCO region (horizontal arrow in Fig. 1) induces SSCOs, as shown in Figs. 4(c) and 4(d). The transient stage between the SS and SSCOs after switching B is due to the formation of a high-field domain at the first QW which travels toward the collector. After the domain reaches the MQWS end, a new high-field domain is formed at the first QW and the same situation is periodically repeated.

IV. DISCUSSION

In this paper, we have systematically analyzed the transition from stationary states to self-sustained current oscillations through a dilute magnetic semiconductor multiquantum well structure. Switching suddenly a control parameter as the (dimensionless) applied voltage ϕ or the external magnetic field B may force the system to move between stable oscillatory and stationary states through the transition region. Since self-sustained current oscillations are caused by triggering high-field domains at the magnetic quantum well, we expect our results not to change qualitatively with the contact boundary condition. We have used two other conditions to check this: (1) $n_0^{\pm}=n_{N+1}^{\pm}=\kappa N_D/2$ in the tunneling currents for

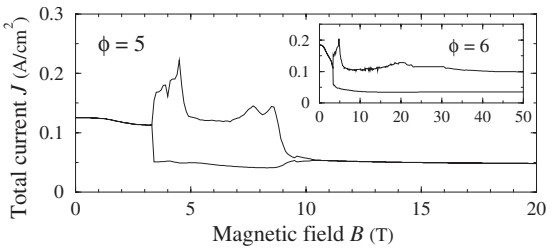

FIG. 3. *J-B* plot for a MQWS with $N=10$ and $\phi=5$. Inset: same for $\phi=6$, showing indefinite persistence of SSCOs for large values of B.

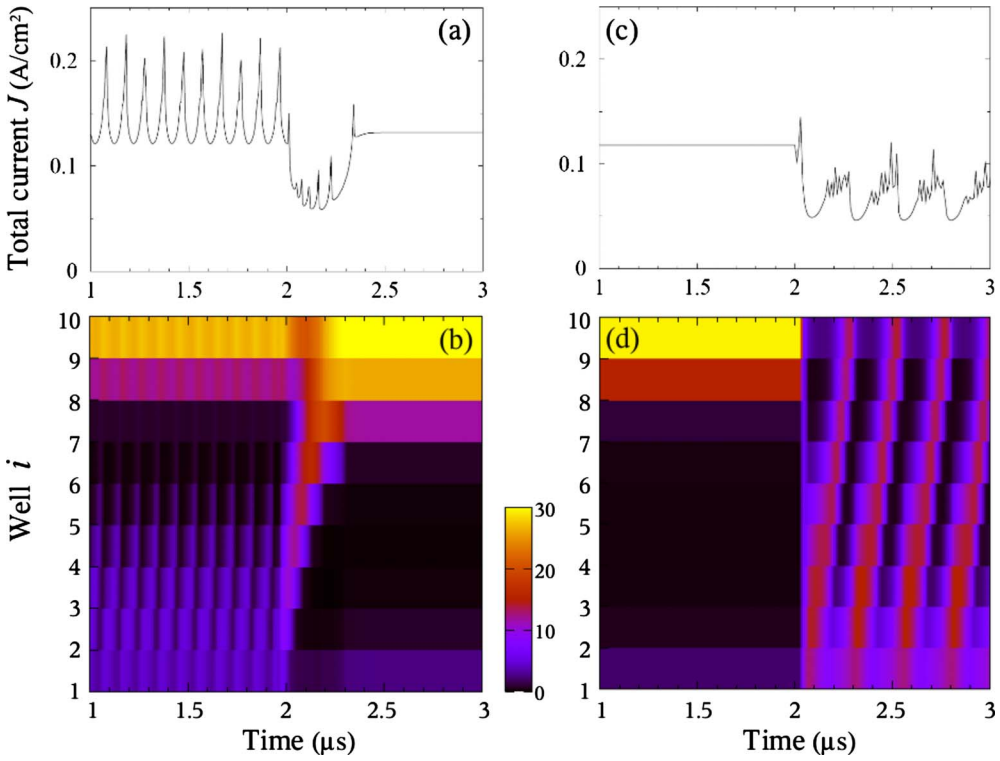

FIG. 4. (Color online) $J(t)$ curve and density plot of the electric field F showing the response of a $N=10$ MQWS to the abrupt switches marked in Fig. 1. (a) and (b): vertical switch from $\phi=7$ to 9 with $\Delta=12$ meV. (c) and (d): horizontal switch from $B=2$ to 6 T with $\phi=5$.

normal contacts, where κ is a positive constant. (2) The electric field at the injector F_0 is calculated by using the Ohm's law,

$$\varepsilon \frac{dF_0}{dt} + \sigma F_0 = J(t). \tag{14}$$

(3) Instead of the tunneling current formulas[14] with known $n_0^{\pm}$.

The resulting phase diagrams for (i) with different values of κ (from 0.5 to 1.5) and for (ii) with different values of the contact resistivity $1/\sigma$ (from 31.3 to 313 Ωm) have the same configuration as in Fig. 1 except for small quantitative shifts of the SSCO regions: increasing κ or $1/\sigma$ enlarges the oscillatory region.

This situation is reminiscent of the early theoretical work on the Gunn effect in bulk GaAs. Gunn's experiments made it clear that the SSCOs in dc voltage biased n-doped GaAs samples are due to the periodic motion of charge dipole waves that appear at the cathode and disappear at the anode.[26] Theorists soon used a variety of boundary conditions at the injecting contact region (cathode) that could produce the required SSCOs mediated by charge dipole waves. Among them, Kroemer's contact characteristics [the electron current density is a known function of the electric field at the contact: in case (ii), this function is linear],[27] general models of metal—semiconductor contacts[28] or contacts with fixed electron density but with a notch near the cathode in the doping density profile.[29] While the two first contact types can give rise to SSCOs mediated by either moving charge dipoles (either high or low electric field domains) or monopoles (either charge accumulation or charge depletion layers) depending on parameter values,[28,30] a notch in the doping density produces only dipoles.[27,29]

While it is feasible to list all possible oscillation types in terms of contact parameter values (see Refs. 28 and 30), these values cannot be modified once the Gunn diode has been made. Similarly, in a conventional III-V weakly coupled n-doped semiconductor superlattice (SL), the boundary condition at the injector, the SL configuration, and the doping density at the QWs determine whether the system exhibits SSCOs mediated by charge dipole or monopole waves[15,16] or multistable static electric field domains; see the review[15] and references cited therein.

In the SL case, there exist partial phase diagrams: (i) doping density vs dc voltage bias for fixed boundary condition[31] and (ii) injector conductivity vs dc voltage bias for fixed doping density (assuming a linear relation between electron current and electric field at the contact).[32] However a complete study (which, depending on both doping density *and* injector conductivity, should yield both monopole and dipole SSCOs, as in Ref. 16) has not yet been carried out. Be this as it may, once the SL has been made and contacted, the stable solutions can be selected only by changing the bias and this limits the type of attractors present in a particular SL.

The situation is different in the case of a dilute magnetic semiconductor multiquantum well structure: the magnetic QW plays the role of a "tunable doping density notch." In principle, any self-oscillations that may appear are due to

triggering of dipoles at the magnetic QW. However, by changing the external magnetic field we can select either stable stationary states or SSCOs as the DMS multiquantum well response.

Our results show how to design a device operating a spin injector and a spin oscillator by tuning the Zeeman splitting and the parameters determining the sample configuration.

ACKNOWLEDGMENTS

Work supported by the MICINN under Grants No. FIS2008-04921-C02-01 and No. MAT2008-02626. R.E. thanks the Spanish Ministry of Education Ramón y Cajal Program.

[1] T. Bland, K. Lee, and S. Steinmüller, Phys. World **21**, 24 (2008).
[2] A. Imamoglu, D. D. Awschalom, G. Burkard, D. P. DiVincenzo, D. Loss, M. Sherwin, and A. Small, Phys. Rev. Lett. **83**, 4204 (1999).
[3] V. Cerletti, O. Gywat, and D. Loss, Phys. Rev. B **72**, 115316 (2005).
[4] M. Titov, B. Trauzettel, B. Michaelis, and C. W. J. Beenakker, New J. Phys. **7**, 186 (2005).
[5] R. Fiederling, M. Keim, G. Reuscher, W. Ossau, G. Schmidt, A. Waag, and L. W. Molenkamp, Nature (London) **402**, 787 (1999).
[6] G. Schmidt, G. Richter, P. Grabs, C. Gould, D. Ferrand, and L. W. Molenkamp, Phys. Rev. Lett. **87**, 227203 (2001).
[7] J. K. Furdyna, J. Appl. Phys. **64**, R29 (1988).
[8] A. Slobodskyy, C. Gould, T. Slobodskyy, G. Schmidt, L. W. Molenkamp, and D. Sánchez, Appl. Phys. Lett. **90**, 122109 (2007).
[9] G. Schmidt, C. Gould, P. Grabs, A. M. Lunde, G. Richter, A. Slobodskyy, and L. W. Molenkamp, Phys. Rev. Lett. **92**, 226602 (2004).
[10] C. Ertler and J. Fabian, Phys. Rev. Lett. **101**, 077202 (2008).
[11] D. Sánchez, A. H. MacDonald, and G. Platero, Phys. Rev. B **65**, 035301 (2001).
[12] M. Béjar, D. Sánchez, G. Platero, and A. H. MacDonald, Phys. Rev. B **67**, 045324 (2003).
[13] L. L. Bonilla, R. Escobedo, M. Carretero, and G. Platero, Appl. Phys. Lett. **91**, 092102 (2007).
[14] R. Escobedo, M. Carretero, L. L. Bonilla, and G. Platero, New J. Phys. **11**, 013033 (2009).
[15] L. L. Bonilla and H. T. Grahn, Rep. Prog. Phys. **68**, 577 (2005).
[16] D. Sánchez, M. Moscoso, L. L. Bonilla, G. Platero, and R. Aguado, Phys. Rev. B **60**, 4489 (1999).
[17] A. Amann, A. Wacker, L. L. Bonilla, and E. Schöll, Phys. Rev. E **63**, 066207 (2001).
[18] L. L. Bonilla, R. Escobedo, and G. Dell'Acqua, Phys. Rev. B **73**, 115341 (2006).
[19] H. Xu and S. W. Teitsworth, Phys. Rev. B **76**, 235302 (2007).
[20] A. Slobodskyy, C. Gould, T. Slobodskyy, C. R. Becker, G. Schmidt, and L. W. Molenkamp, Phys. Rev. Lett. **90**, 246601 (2003).
[21] J. Bardeen, Phys. Rev. Lett. **6**, 57 (1961).
[22] L. Brey, G. Platero, and C. Tejedor, Phys. Rev. B **38**, 9649 (1988).
[23] L. Brey, G. Platero, and C. Tejedor, Phys. Rev. B **38**, 10507 (1988).
[24] G. Platero, L. Brey, and C. Tejedor, Phys. Rev. B **40**, 8548 (1989).
[25] L. L. Bonilla, J. Phys.: Condens. Matter **14**, R341 (2002).
[26] J. B. Gunn, in *Proceedings of the Symposium on Plasma Effects in Solids*, edited by J. Bok (Dunod, Paris, 1965), p. 199.
[27] H. Kroemer, IEEE Trans. Electron Devices **15**, 819 (1968).
[28] G. Gomila, J. M. Rubí, I. R. Cantalapiedra, and L. L. Bonilla, Phys. Rev. E **56**, 1490 (1997).
[29] D. E. McCumber and A. G. Chynoweth, IEEE Trans. Electron Devices **13**, 4 (1966).
[30] F. J. Higuera and L. L. Bonilla, Physica D **57**, 161 (1992).
[31] J. Galán, L. L. Bonilla, and M. Moscoso, SIAM J. Appl. Math. **60**, 2029 (2000).
[32] J. Hizanidis, A. Balanov, A. Amann, and E. Schöll, Phys. Rev. Lett. **96**, 244104 (2006).